Warranty Prediction Based on Auxiliary Use-rate Information

Yili Hong and William Q. Meeker
Department of Statistics
Iowa State University
Ames, IA, 50011

Abstract

Usually the warranty data response used to make predictions of future failures is the number of weeks (or another unit of real time) in service. Use-rate information usually is not available (automobile warranty data are an exception, where both weeks in service and number of miles driven are available for units returned for warranty repair). With new technology, however, sensors and smart chips are being installed in many modern products ranging from computers and printers to automobiles and aircraft engines. Thus the coming generations of field data for many products will provide information on how the product has been used and the environment in which it was used. This paper was motivated by the need to predict warranty returns for a product with multiple failure modes. For this product, cycles-to-failure/use-rate information was available for those units that were connected to the network. We show how to use a cycles-to-failure model to compute predictions and prediction intervals for the number of warranty returns. We also present prediction methods for units not connected to the network. In order to provide insight into the reasons that use-rate models provide better predictions, we also present a comparison of asymptotic variances comparing the cycles-to-failure and time-to-failure models.

Key Words: Calibration; Cycles to failure; Multiple failure modes; Prediction intervals; Product reliability.

1 Introduction

1.1 Background

Traditional reliability data have consisted of failure times for units that failed and running times for units that had not failed. Although laboratory reliability testing is often used to make product design decisions, the "real" reliability data come from the field, often in the form of warranty returns (for consumer products) and field tracking studies (e.g., for company-owned assets and medical devices). The field data often exhibit more variability in component or product failure times than the data from the laboratory testing. This important difference between carefully controlled laboratory accelerated test experiments and field reliability results is due to uncontrolled field variation (unit-to-unit and temporal) in variables, such as use rate, load, vibration, temperature, humidity, UV intensity, and UV spectrum. Thus, incorporating use-rate/environmental data into our analyses can be expected to explain one important source of variability and provide stronger statistical methods and more accurate inferences or predictions. Historically, however, use-rate/environmental information on individual units has, in most applications, not been available to reliability analysts.

The future generations of reliability field data will be richer in use-rate/environmental information. For example, today, it is possible to install sensors and smart chips in a product to measure and record use-rate/environmental data over the life of the product. This information is available at the time of product return/repair. For products that are connected to network or installed with a wireless transmission device, such information can be available dynamically or periodically.

Products for which use-rate information is available dynamically include products that are connected to the network (e.g., computers and high-end printers) or other communications channels. Such data can, in cooperation with the owner, be downloaded periodically. The use rate might be number of hours that power is on for a computer or the number of pages printed for a printer.

1.2 Applications in Prediction

The main focus of this paper is to develop methods to take advantage of auxiliary use-rate information, when it is available on some or all of the units in a product population, to obtain better predictions of future warranty costs for a product. Use-rate information can be of great advantage in reliability applications. In particular,

- Many life-limiting failure modes depend more or less directly on the amount of product use. For example, the failure time of a computer disk drive would be expected to related

to the number of hours that the disk had been used. If time to failure is measured in weeks of service and if there is variability in the number of hours per week the disk drive is used, there will be more variability in the failure-time data and less precision in failure-time prediction.

- Prediction models based on the amount of product use will generally be more accurate when predicting the failure times of individual units or the cumulative number of future failures for the population. The fraction failing for products over the observation period (e.g., one year) is typically small (e.g., less than 1% or 2%). Hence, the amount of extrapolation is large when doing prediction based on time-to-failure data. Cycles-to-failure data, however, allow us to have observations with a large number of cycles for units that were heavily used. Thus, the effective amount of extrapolation is smaller when doing prediction based on cycles-to-failure data. See Section 5 for more details.

For the units of a product in the field, it is possible that only part of the population is connected to the network. For the connected population, use-rate information is available. For the not-connected population, use-rate information is not available. Two specific problems arise in application.

- How to predict the number of warranty returns for the connected population, taking advantage of the use-rate information.

- How to make similar predictions for the not-connected population using use-rate information from the connected population.

1.3 Product D Example

Our example is based on an application involving what we will call Product D. Product D is used in offices or residences. To protect sensitive proprietary information, we have had to change the names of the product, use coded names for different failure modes, and simulate data based on the actual model that was used to describe the data. The use-rate (number of cycles of use per week where a cycle is a specific amount of product use, such as the typical amount of use in a day) information can be downloaded through a network if the unit is connected to the network. As an analogy, Product D can be thought of as a copying machine with a smart chip to record the number of pages that have been printed, as a function of time.

1.4 Related Literature

Lawless (1998) provides a general review of methods for product warranty data analyses and describes some extensions and suggestions for future work. For statistical methodology and

applications related to product use, Yang (2007, Section 11.5) discusses simple models for usage accumulation rate. Lawless, Crowder, and Lee (2009) present models that can be used to assess the dependence of warranty claims on time in service or usage of a product, and parameter estimations based on different types of field data. However, the product use information was only available for returned units. In this paper, we have product use information both for returned and in-service units for the connected population. Meeker, Escobar, and Hong (2009) developed models and methods for using both the field data and accelerated life test data to estimate the field use-rate information which were used to do predict the failure-time distribution for new designed products.

In the area of prediction intervals (PI), Komaki (1996) and Barndorff-Nielsen and Cox (1996) studied calibration of the naive "plug-in" PI procedure to account for statistical uncertainty by using asymptotic expansions. Beran (1990), Meeker and Escobar (1998, Chapter 12), and Escobar and Meeker (1999) studied calibration of a naive PI using Monte Carlo simulation/bootstrap re-sampling methods for relatively simple situations. Lawless and Fredette (2005) showed how to use a predictive distribution approach to provide a PI procedure that is the same as the calibrated naive PI. Hong, Meeker, and McCalley (2009) developed PI procedures and associated calibration methods for a more complicated reliability prediction problem involving regression analysis of left truncation and right censored failure-time data. A PI procedure for multiple failure modes, however, has not been treated in the literature. David and Moeschberger (1978), and Crowder (2001) are useful books on the subject of competing risks models and sub-distribution functions. These models are useful for modeling and predicting in reliability applications with multiple failure modes.

2 Data and Failure-time Models Based on Product Use

2.1 Product D Data

The population of Product D units in the field can be divided into two groups:

- For units *not connected* to the network, we have the traditional failure-time data, containing information on time to failure (time in service) for failed (censored) units. For Product D, the time scale is weeks. Failure mode information is also available for returned units.

- For units *connected* to the network, we were also provided with data consisting of cycles to failure (cycles in service) for failed (censored) units as well as the average number of cycles per week for each unit, over its period of observation.

The data were multiply censored due to staggered entry of product into the field over time. In automobile warranty data, the amount of use (miles driven) is available only for those units that are returned for service (e.g., Kalbfleisch, Lawless, and Robinson 1991). For Product D, we have such information for all units that are connected to the network obtained by taking a snapshot of the dynamic use-rate data at the data-freeze date (DFD). Although it was technically possible to obtain the dynamic use-rate data as a time series giving the number of cycles of use for each day, for our prediction task only the use rate for each unit at the DFD was provided. This information was summarized by the cumulative number of cycles divided by the number of weeks in service.

We use data up to end of the warranty period which, for Product D, is two years (104 weeks). That is, if a unit is returned for service after the warranty period, we treat the unit as being censored at the end of the warranty period. We do this because it was believed that only a fraction of units that fail after the end of the warranty period would be returned to the manufacturer for service. Thus using failures after the warranty period would bias estimates of the failure-time distribution.

Product D fails from causes that can be categorized into one of four major failure mode groups, which are coded as failure mode 1 (FM1), failure mode 2 (FM2), failure mode 3 (FM3), and all other failure modes (FMOther). The failure mode can be determined by the repair technician when the product is returned for repair warranty. From engineering knowledge and because of the manner in which the failure mode grouping was done, it is reasonable to assume that the cycles-to-failure random variables for these four failure mode groups are independent.

2.2 Motivation for Multiple Failure Modes Analysis

For Product D (and many other products), it was important to use failure mode information in estimation and prediction. The reasons for this were:

- When the failure modes behave differently (e.g., some are defect or infant mortality related and others are caused by wearout), it is generally easier to find a well fitting distribution to the individual failure modes (e.g., Device G in Example 15.6 from Meeker and Escobar 1998).

- When forecasting warranty costs, some failure modes are much more expensive to fix than others (e.g., replacing a mother board in a computer versus replacing a defective battery). In some applications, there is one failure mode that is of critical importance (e.g., a failure mode that could cause serious harm) and others that are innocuous leading to end of life of the product and thus eliminating the possibility of the critical failure mode.

Population	Number of failures					Censored	Total
	FM1	FM2	FM3	FMOther	total		
Connected	9	37	22	6	74	912	986
Not-connected	9	40	32	7	88	1038	1126

Table 1: Summary of the Product D data

- Predictions are often needed for the number of replacement parts that will be needed to effect repairs and different failure modes require different parts.
- Knowledge of the relative frequency of different failure modes and the effect of eliminating one or more of the individual failure modes is important for engineers who need to make design changes that will improve product reliability and reduce future warranty costs.

2.3 Notation

The cycles-to-failure data from the connected population are denoted by $(c_i, r_i, \delta_{ki}; k = 1, \cdots, K)$, $i = 1, 2, \cdots, n$. Here, c_i is the observed cycles to failure (cycles in service) for the failed (censored) units. Let t_i be the observed weeks to failure (weeks in service) for the failed (censored) units. The observed use rate r_i can be obtained as $r_i = c_i/t_i$. δ_{ki} is the observed failure indicator for failure mode k; $\delta_{ki} = 1$ and $\delta_{li} = 0$ for $l \neq k$ if unit i failed due to failure mode k and $\delta_{ki} = 0$ for all k if unit i had not failed (censored). K denotes the number of failure modes ($K = 4$ for the Product D data) and n is the number of observations in the connected population. The time-to-failure data from the not-connected population are denoted by $(t_j, \delta_{kj}; k = 1, \cdots, K), j = 1, 2, \cdots, m$ where m is the number of observations in not-connected population.

2.4 Log-location-scale Distributions

Log-location-scale distributions are often used to model the failure-time distribution of products. The cumulative distribution function (cdf) of a random variable T with a distribution from the log-location-scale family is

$$F(t; \boldsymbol{\theta}) = \Phi\left[\frac{\log(t) - \mu}{\sigma}\right] \tag{1}$$

where $\boldsymbol{\theta} = (\mu, \sigma)'$, μ is the location parameter and σ is the scale parameter for $\log(T)$. Correspondingly, $\exp(\mu)$ and σ are scale and shape parameter respectively, for T. Here $\Phi(\cdot)$

is the standard cdf for the location-scale family of distributions ($\mu = 0$ and $\sigma = 1$). The corresponding probability density function (pdf) is

$$f(t;\boldsymbol{\theta}) = \frac{1}{\sigma t}\phi\left[\frac{\log(t)-\mu}{\sigma}\right] \tag{2}$$

where $\phi(\cdot)$ is the standard pdf for the location-scale family of distributions. The cdf and pdf of the Weibull random variable can be obtained by replacing $\Phi(\cdot)$ in (1) and $\phi(\cdot)$ in (2) with $\Phi_{\text{sev}}(z) = 1 - \exp[-\exp(z)]$ and $\phi_{\text{sev}}(z) = \exp[z - \exp(z)]$, respectively. The cdf and pdf of a lognormal random variable can be obtained similarly using the standard normal cdf and pdf, respectively. The Weibull and the lognormal distributions are the most commonly used distributions for describing failure time in reliability applications. It is worth pointing out that the models and methodology used in this paper can be extended to other distributions. For the Product D data, however, the log-location-scale family of distributions was all that was needed.

2.5 Competing Risks and Cycles-to-failure Models

Let C_k be the cycles to failure for failure mode $k, k = 1, 2, \cdots, K$. The marginal cdf of C_k is denoted by $F_{C_k}(c;\boldsymbol{\theta}_{C_k})$ where $\boldsymbol{\theta}_{C_k} = (\mu_{C_k}, \sigma_{C_k})'$. Because Product D is a series system, the cycles to failure of the product is $C = \min\{C_1, C_2, \cdots, C_K\}$. Let Δ_k be the failure indicator for failure mode k. $\Delta_k = 1$ and $\Delta_l = 0$ for $l \neq k$ if a unit failed due to failure mode k. $\Delta_l = 0$ for all l if the unit had not failed (i.e., the failure time were censored). In this case, C is the cycles in service of the product.

Because all C_k's are independent, the cycles-to-failure cdf of C is

$$F_C\left(c;\boldsymbol{\theta}_C\right) = 1 - \prod_{k=1}^{K}\left[1 - F_{C_k}(c;\boldsymbol{\theta}_{C_k})\right]$$

where $\boldsymbol{\theta}_C = \left(\boldsymbol{\theta}'_{C_1}, \boldsymbol{\theta}'_{C_2}, \cdots, \boldsymbol{\theta}'_{C_K}\right)'$.

2.6 Use-rate Distribution and Time-to-failure Models

Let R be the use rate for a unit that is connected to the network. The distribution of R, across units in the population, is denoted by F_R. In this application, we found that the use-rate distribution could not be described by a simple distribution. This is because use rate is related to a mixture of customer use behaviors. Thus we do not assume a parametric distribution for R. Instead, we use a simple nonparametric estimate. Figure 1 gives a histogram of the use rate for the connected units.

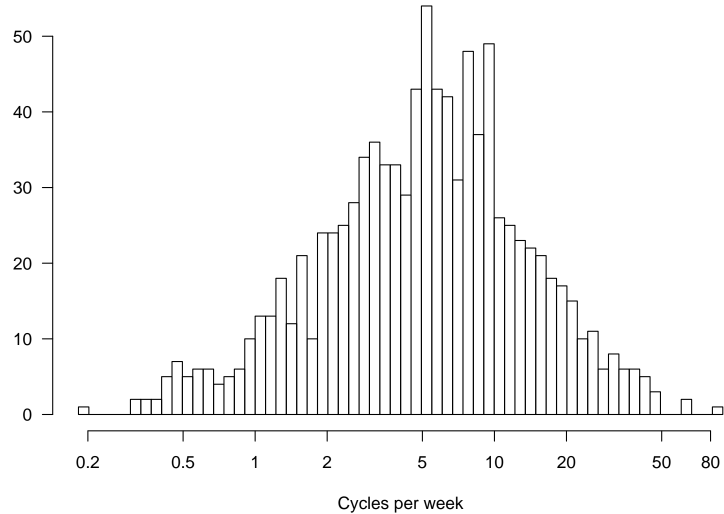

Figure 1: Histogram of use rate for the connected units

Let T_k be the time to failure for failure mode k, $k = 1, 2, \cdots, K$. The time to failure of the product is $T = \min\{T_1, T_2, \cdots, T_K\}$, where Δ_k's are the failure indicators as defined in Section 2.5. T is also used to denote the time in service for unfailed units.

Because R is the use rate, $T = C/R$. For Product D, the use rate is related to customer use behaviors and cycles to failure depends on the product component failure mechanisms. Because the amount of customer use would not depend on component failure times, it is reasonable to assume that C_k's and R are independent in our model. For other products, it is possible that C_k and R could be dependent. For example, if a toaster is used repeatedly without cooling down, the higher than usual temperature could cause the cycles-to-failure distribution to depend on the use rate. In this case, an appropriate model should be considered. For example, the power-rule relationship can be used to describe how use rate affects the cycles to failure distribution (see, Escobar and Meeker 2006, Section 4.2 for more details). We also assume that customer use rate is constant over time. This assumption is particularly important for prediction and can be checked by periodically downloading use-rate information from connected units.

Under the assumption of independence of R and C_k, the marginal cdf of T_k is

$$F_{T_k}(t; \boldsymbol{\theta}_{C_k}, F_R) = \int_0^\infty F_{C_k}(rt; \boldsymbol{\theta}_{C_k})\, dF_R(r).$$

The distribution of T_k is not, in general, a member of the log-location-scale family. Also, because of unit-to-unit variability in R, the $T_k, k = 1, 2, \cdots, K$, are not independent. The cdf

of the time to failure, T is

$$F_T\,(t;\boldsymbol{\theta}_T) = \int_0^\infty F_C(rt;\boldsymbol{\theta}_C)\,dF_R(r)$$

where $\boldsymbol{\theta}_T = \{\boldsymbol{\theta}_C, F_R\}$ is the collection of parameters for the distribution of T.

The sub-distribution function of the cycles to failure for failure mode k is

$$\begin{aligned} F_C(k, c;\boldsymbol{\theta}_C) =& \Pr(\Delta_k = 1, C \le c) = \Pr(C_k \le c, C_l > C_k;\ \text{for all } l \ne k) \\ =& \int_0^c f_{C_k}(c_k;\boldsymbol{\theta}_{C_k}) \prod_{l\ne k} [1 - F_{C_l}(c_k;\boldsymbol{\theta}_{C_l})]\, dc_k \end{aligned}$$

and gives the fraction failing due to failure mode k. Note that $F_C(c;\boldsymbol{\theta}_C) = \sum_{k=1}^K F_C(k,c;\boldsymbol{\theta}_C)$. See, for example, Crowder (2001, page 46) for more details. Similarly, the sub-distribution function of the time to failure for failure mode k is

$$F_T(k,t;\boldsymbol{\theta}_T) = \Pr(\Delta_k = 1, T \le t) = \int_0^\infty F_C(k, rt;\boldsymbol{\theta}_C) dF_R(r).$$

Note that $F_T(t;\boldsymbol{\theta}_T) = \sum_{k=1}^K F_T(k,t;\boldsymbol{\theta}_T)$.

3 Maximum Likelihood Estimation for the Failure-time Distribution Parameters

3.1 Estimating the Parameters for the Connected Population

We use the cycles-to-failure data to estimate the parameters for the connected population. The likelihood of the cycles-to-failure data is

$$L_{CTF}(\boldsymbol{\theta}_C|DATA) = \prod_{k=1}^K L(\boldsymbol{\theta}_{C_k}|DATA) \tag{3}$$

where $L(\boldsymbol{\theta}_{C_k}|DATA) = \prod_{i=1}^n \left\{[f_{C_k}(c_i;\boldsymbol{\theta}_{C_k})]^{\delta_{ki}}\,[1 - F_{C_k}(c_i;\boldsymbol{\theta}_{C_k})]^{(1-\delta_{ki})}\right\}$. The maximum likelihood (ML) estimator is denoted by $\widehat{\boldsymbol{\theta}}_C$ and can be obtained by maximizing (3). The nonparametric ML estimator of F_R is the empirical cdf, denoted by $\widehat{F}_R(r) = n^{-1}\sum_{i=1}^n \mathbf{1}_{(r_i \le r)}$ where $\mathbf{1}_{(\cdot)}$ is the indicator function.

Figure 2 is a cycles-to-failure lognormal probability plot for all of the failure modes, also showing ML estimates for the cycles-to-failure marginal distributions for each failure mode. The points in Figure 2 were plotted at each of the observed failures and at the corresponding midpoint of the step of the Kaplan-Meier (KM) cdf estimates, as suggested in Lawless (2003, Section 3.3). The distribution chosen for FM1, FM3 and FMOther was lognormal, and for

FM	parameter	ML estimate	standard error	95% approximate CI	
				lower	upper
FM1	μ_{C_1}	8.222	0.269	7.695	8.748
	σ_{C_1}	0.743	0.138	0.517	1.068
FM2	μ_{C_2}	9.401	0.449	8.521	10.281
	σ_{C_2}	1.109	0.141	0.864	1.423
FM3	μ_{C_3}	20.870	3.057	14.878	26.862
	σ_{C_3}	7.677	1.448	5.305	11.110
FMOther	μ_{C_4}	10.627	1.223	8.230	13.025
	σ_{C_4}	1.871	0.507	1.100	3.183

Table 2: ML estimates and approximate confidence interval (CI) for parameters for the connected population.

FM2 was the Weibull. Note that the plot of the Weibull ML estimate for FM2 is a curve in Figure 2. In the analysis of the real data, we explored the use of different distributions for different failure modes. We compared the model fit results by looking at the probability plots for the individual failure modes, ending with results like those shown in Figure 2, providing a good fit to the data. Table 2 gives the ML estimates, standard errors and 95% approximate confidence intervals for the model parameters. Figure 3 shows the lognormal probability plot of the system failure times along with the ML estimate of the series system failure time cdf. The ML estimates of the sub-distribution functions (which sum to the series system estimate) are also shown for the connected population. The parametric estimate of the cdf of the series system agrees well with the KM estimates.

3.2 Estimating Parameters for the Not-connected Population

For Product D, it is reasonable to assume that the two populations (connected and not) have the same cycles-to-failure distributions for each failure mode. This because these units are of the same design and were manufactured in the same plants. The difference in the distributions of time to failure in these two populations, if any, is due to the differences between the use-rate distributions of the two populations. It is impossible to get an estimate of the use-rate distribution based only on the data from the not-connected population. Combining data from the connected and not-connected populations, however, will allow us to estimate the use-rate distribution for the not-connected population. Doing this requires some model assumptions.

For Product D, we assume that the use rate for the not-connected population is τR where R is the use rate for the connected population and τ is an unknown positive factor. This assumption allows us to connect the distribution of the time to failure for the connected

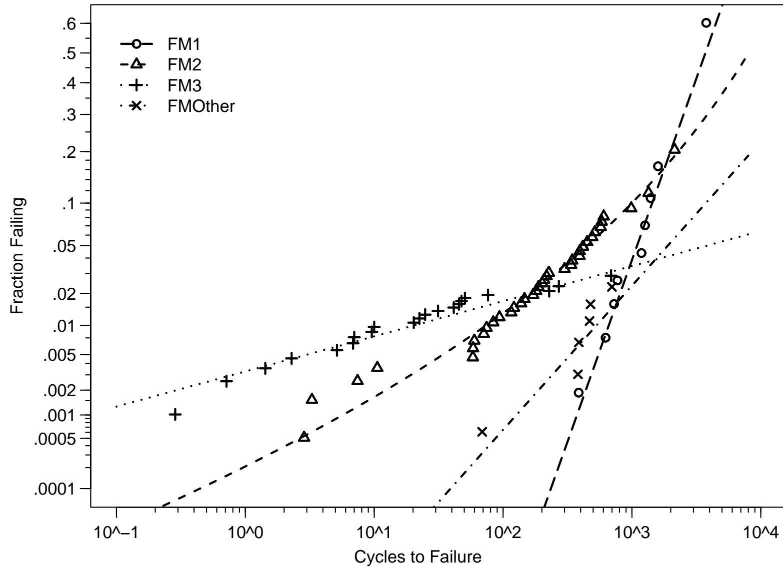

Figure 2: Lognormal probability plot for cycles to failure for all failure modes, showing the corresponding ML estimates of the marginal cdfs for the connected population.

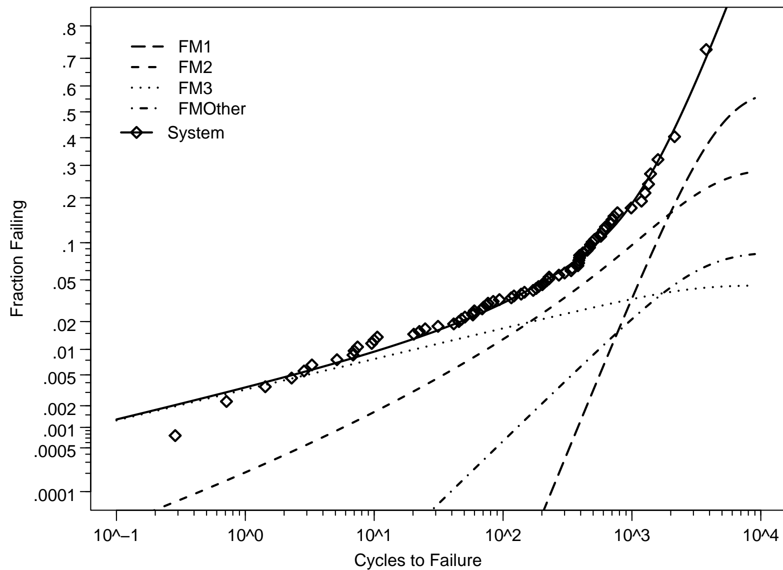

Figure 3: Lognormal probability plot of the system failure times along with the ML estimate of the series system failure-time cdf for the connected population. The ML estimates of the sub-distribution functions are also shown.

and not-connected populations. The parameter for the not-connected population is denoted by $\boldsymbol{\theta}_T = \{\boldsymbol{\theta}_C, F_{\tau R}\}$. The ML estimate of $\widehat{\boldsymbol{\theta}}_T$ is obtained by the following procedure. We start with the nonparametric ML estimator of $F_{\tau R}$, given τ. This estimator is $\widehat{F}_{\tau R}(r) = n^{-1}\sum_{i=1}^{n} \mathbf{1}_{(\tau r_i \leq r)} = n^{-1}\sum_{i=1}^{n} \mathbf{1}_{(r_i \leq r/\tau)}$. The likelihood of the combined data (connected and not-connected) given $\widehat{F}_{\tau R}$ is

$$L(\boldsymbol{\theta}_C, \widehat{F}_{\tau R}|DATA) = L_{CTF}(\boldsymbol{\theta}_C|DATA) \times L_{TIS}(\boldsymbol{\theta}_C, \widehat{F}_{\tau R}|DATA). \tag{4}$$

Here, $L_{CTF}(\boldsymbol{\theta}_C|DATA)$ is in (3) and

$$\begin{aligned} L_{TIS}(\boldsymbol{\theta}_C, \widehat{F}_{\tau R}|DATA) = & \prod_{j=1}^{m} \left\{ \left(\prod_{k=1}^{K} \left[A_{kj}(t_j; \boldsymbol{\theta}_C, \widehat{F}_{\tau R}) \right]^{\delta_{kj}} \right) \right. \\ & \left. \times \left[1 - F_T(t_j; \boldsymbol{\theta}_C, \widehat{F}_{\tau R}) \right]^{\prod_{k=1}^{K}(1-\delta_{kj})} \right\} \end{aligned}$$

where $A_{kj}(t_j; \boldsymbol{\theta}_C, \widehat{F}_{\tau R}) = \int_0^\infty r f_{C_k}(rt_j; \boldsymbol{\theta}_{C_k}) \prod_{l \neq k}[1 - F_{C_l}(rt_j; \boldsymbol{\theta}_{C_l})] d\widehat{F}_{\tau R}(r)$. $A_{kj}(t; \boldsymbol{\theta}_C, F_{\tau R})$ is proportional to the probability of observing a unit failing due to failure mode k between time t and $t + dt$, where dt is an infinitesimal amount of time. $1 - F_T(t_j; \boldsymbol{\theta}_C, \widehat{F}_{\tau R})$ gives the probability of observing a unit that has not failed before time t. The ML estimator obtained by maximizing (4) is denoted by $\left\{\widehat{\boldsymbol{\theta}}_C, \widehat{\tau}\right\}$. Thus, the ML estimator of $\boldsymbol{\theta}_T$ for the weeks to failure distribution is $\widehat{\boldsymbol{\theta}}_T = \left\{\widehat{\boldsymbol{\theta}}_C,\ \widehat{F}_{\widehat{\tau} R}\right\}$ where $\widehat{F}_{\widehat{\tau} R}(r) = \sum_{i=1}^{n} \mathbf{1}_{(r_i \leq r/\widehat{\tau})}$.

Figures 4 and 5 are similar to Figures 2 and 3 but for the not-connected population. The parametric estimates for the not-connected population displayed in Figures 4 and 5 also agree well with the nonparametric ones. Table 3 is similar to Table 2, except that it contains an estimate of τ.

There is an alternative to estimate $\{\boldsymbol{\theta}_C, \tau\}$. One can use $\widehat{\boldsymbol{\theta}}_C$ obtained by maximizing (3) as the estimate of $\boldsymbol{\theta}_C$ and obtain $\widehat{\tau}$ by maximizing (4) with $\boldsymbol{\theta}_C$ fixed at $\widehat{\boldsymbol{\theta}}_C$. The ML estimator $\left\{\widehat{\boldsymbol{\theta}}_C, \widehat{\tau}\right\}$ obtained by maximizing (4), however, would be expected to have better statistical properties because both data from connected population and not-connected population are used in the estimation of $\boldsymbol{\theta}_C$.

4 Predictions Based on a Product Use Model

As described in Section 2.1, the goal of our analysis was to predict the cumulative number of warranty returns for each failure mode, as a function of time, based on the currently available data. PIs are also needed for quantifying the statistical uncertainties. The predictions need to correspond to real time, after the data-freeze date (DFD).

The predictions are based on the distribution of remaining life of units that survived until the DFD. The remaining life of unit i is the amount of time to failure after the DFD,

FM	parameter	ML estimate	standard error	95% approximate CI lower	95% approximate CI upper
FM1	μ_{C_1}	8.293	0.263	7.776	8.809
	σ_{C_1}	0.775	0.135	0.550	1.092
FM2	μ_{C_2}	9.436	0.353	8.744	10.127
	σ_{C_2}	1.114	0.109	0.919	1.351
FM3	μ_{C_3}	25.737	2.622	20.598	30.875
	σ_{C_3}	10.414	1.271	8.198	13.229
FMOther	μ_{C_4}	11.316	1.224	8.917	13.715
	σ_{C_4}	2.183	0.511	1.380	3.454
	τ	1.024	0.151	0.767	1.367

Table 3: ML estimates and approximate CI for parameters for the not-connected population.

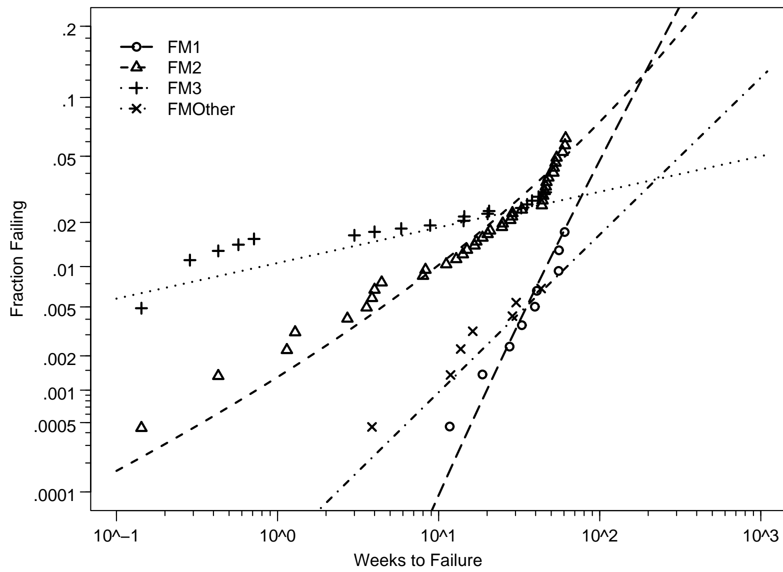

Figure 4: Lognormal probability plot for ML estimates for each failure mode for the not-connected population.

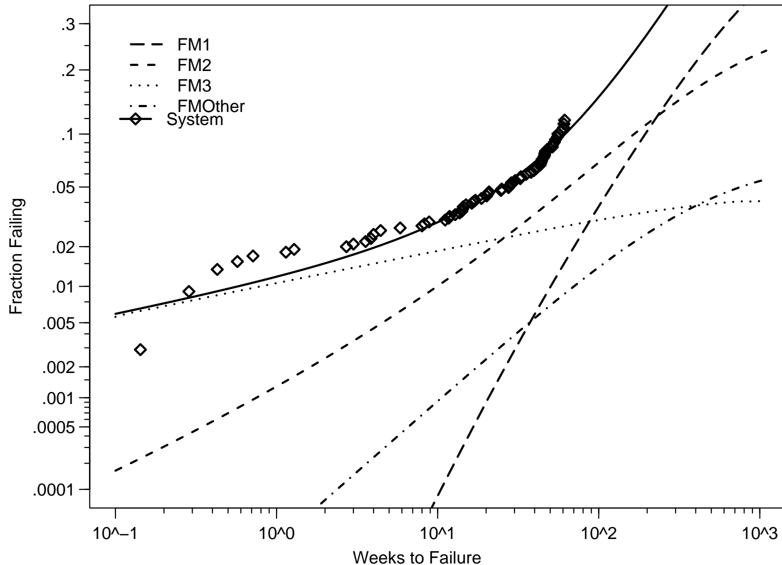

Figure 5: Lognormal probability plot of the system failure times along with the ML estimate of the series system failure-time cdf for the not-connected population. The ML estimates of the sub-distribution functions for the not-connected population are also shown.

conditional on having survived until the DFD. The distribution of remaining life of unit i is the failure probability distribution of $T - t_i$ given its current time in service t_i. The distribution of remaining life provides the basis for calculating the prediction of the cumulative number of failure at a specified point in future time.

4.1 Prediction for the Connected Population

For the connected population (where direct use-rate information is available), the predictions are conditional on the observed time in service (t_i) and the observed use rate (r_i) for each unit and are based on the ML estimators given in Section 3.1.

4.1.1 Prediction for the Number of Returns for Each Failure Mode

The sub-hazard function for unit i at s time units (e.g., weeks) after the DFD due to failure mode k, conditional on the unit surviving until t_i and having use rate r_i, is

$$\nu_{ki}(s) = \lim_{\Delta s \to 0} \frac{\Pr(\Delta_{ki} = 1, t_i + s < T_i \leq t_i + s + \Delta s | T_i > t_i, R_i = r_i)}{\Delta s}.$$

We only do prediction for units until the end of their warranty period. If $t_i + s > w$ (w is the length of the warranty period), the unit is no longer in the risk set. Hence, the warranty-

period-adjusted conditional failure probability of unit i failing due to failure mode k, at s time units after the DFD, is

$$\rho_{ki}(s) = \int_0^s \nu_{ki}(u)\mathbf{1}_{(t_i+u\leq w)}du = \Pr(\Delta_{ki}=1, T_i \leq t_i^w | T_i > t_i, R_i = r_i).$$

Here, $t_i^w = \min\{t_i + s, w\}$. In particular,

$$\begin{aligned}\rho_{ki}(s) &= \Pr(C_{ki} \leq r_i t_i^w, C_{li} > C_{ki};\ \text{for all } l \neq k | C_i > r_i t_i, R_i = r_i) \\ &= \frac{F_C(k, r_i t_i^w; \boldsymbol{\theta}_C) - F_C(k, r_i t_i; \boldsymbol{\theta}_C)}{1 - F_C(r_i t_i; \boldsymbol{\theta}_C)}, \quad k = 1, \cdots, K.\end{aligned} \tag{5}$$

Note that ρ_{ki} is a function of $s > 0$. We omit the argument s in the rest of the paper for notational simplicity. The ML estimator of ρ_{ki}, denoted by $\widehat{\rho}_{ki}$, can be obtained by substituting the ML estimates $\widehat{\boldsymbol{\theta}}_C$ into (5).

The cumulative number of future warranty returns due to failure mode k at s time units after the DFD is $N_k = \sum_{i \in RS} I_{ki}$, where $I_{ki} \sim \text{Bernoulli}(\rho_{ki})$, $i \in RS$, where RS is the risk set at the DFD. That is, RS is a collection of units that have not failed and with $t_i < w$ at the DFD. Note that the N_k's are not independent. The total number of returns at s time units after the DFD is $N = \sum_{k=1}^K N_k$.

Figure 6(a) shows predicted returns per week after the DFD due to each failure mode for the connected population under the assumption that units remain in the risk set until failure (no limit on the warranty period). These predictions reflect the actual costs to customers for their products. Figure 6(b) shows the predicted number of returns per week under the assumption that the units leave the risk set at the end of their two-year warranty period. The predictions are not smooth because of the staggered entry of units into service over time. These predictions are related to the warranty cost for the manufacturer and the amount of effort that will be required at the warranty repair shop. Figure 7 shows the predicted cumulative number of returns as a function of time for each failure mode for the connected population.

4.1.2 Prediction Intervals for Individual Failure Modes and Calibration

Denote the PI by $\left[\underset{\sim}{N}_k,\ \widetilde{N}_k\right]$, $k = 1, \cdots, K$. The naive (plug-in) PI can be obtained by solving

$$F_{N_k}(\underset{\sim}{N}_k; \widehat{\boldsymbol{\theta}}_C) = \frac{\alpha}{2}, \quad \text{and} \quad F_{N_k}(\widetilde{N}_k; \widehat{\boldsymbol{\theta}}_C) = 1 - \frac{\alpha}{2}, \quad k = 1, 2, \cdots, K, \tag{6}$$

where $F_{N_k}(n_k; \boldsymbol{\theta}_C), n_k = 0, 1, \cdots, n^*$ is the cdf of N_k and n^* is the number of units in the RS at the DFD. Note that the cdf of N_k does not have a simple closed-form expression. In a similar prediction application, Hong, Meeker, and McCalley (2009) used an approximation suggested by Volkova (1996). The Volkova approximation is also used here. In particular, the cdf of N_k can be approximated by $F_{N_k}(n_k; \boldsymbol{\theta}_C) = G\left\{[n_k + .5 - \mu(\boldsymbol{\theta}_C)]/\sigma(\boldsymbol{\theta}_C); \boldsymbol{\theta}_C\right\}$, where $G(x, \boldsymbol{\theta}_C) =$

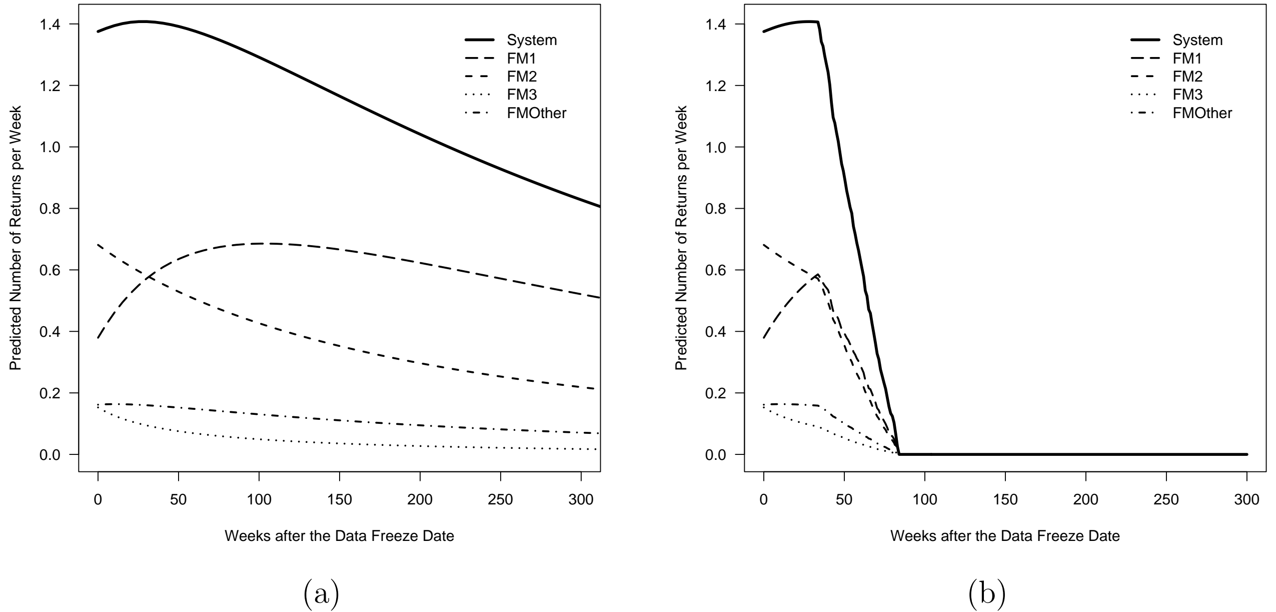

Figure 6: (a) The predicted number of returns per week after the DFD due to each failure mode for the connected population assuming the length of the warranty period is infinity. (b) Similar results but the warranty period is two years.

$\Phi_{\text{nor}}(x) + \gamma(\boldsymbol{\theta}_C)(1 - x^2)\phi_{\text{nor}}(x)/6$, and $\mu(\boldsymbol{\theta}_C) = \sum_{i \in RS} \rho_{ki}$, $\sigma(\boldsymbol{\theta}_C) = \left[\sum_{i \in RS} \rho_{ki}(1 - \rho_{ki})\right]^{1/2}$, $\gamma(\boldsymbol{\theta}_C) = \sigma^{-3}(\boldsymbol{\theta}_C) \sum_{i \in RS} \rho_{ki}(1-\rho_{ki})(1-2\rho_{ki})$ are the mean, standard deviation, and skewness of the distribution of N_k, respectively. As described in Escobar and Meeker (1999, Section A.3), the Poisson approximation can be used if the expected number of returns is small (e.g., less than 5).

The naive PI procedure ignores the uncertainty in $\widehat{\boldsymbol{\theta}}_C$ and thus the coverage probability (CP) is expected to be smaller than the nominal CP. Thus, the naive PI needs to be calibrated. The calibration procedure in Hong, Meeker, and McCalley (2009) can be extended to the multiple failure mode prediction needed here. We describe the procedure in the appendix (**Procedure P1** of Appendix A).

4.1.3 Simultaneous Prediction Intervals for Individual Failure Modes and Calibration

In practice, it is useful to plot the cumulative number of returns caused by each failure mode at a specific future time and compare them simultaneously over all failure modes. Simultaneous prediction intervals (SPIs) are useful for this purpose. The SPIs for multiple failure modes at

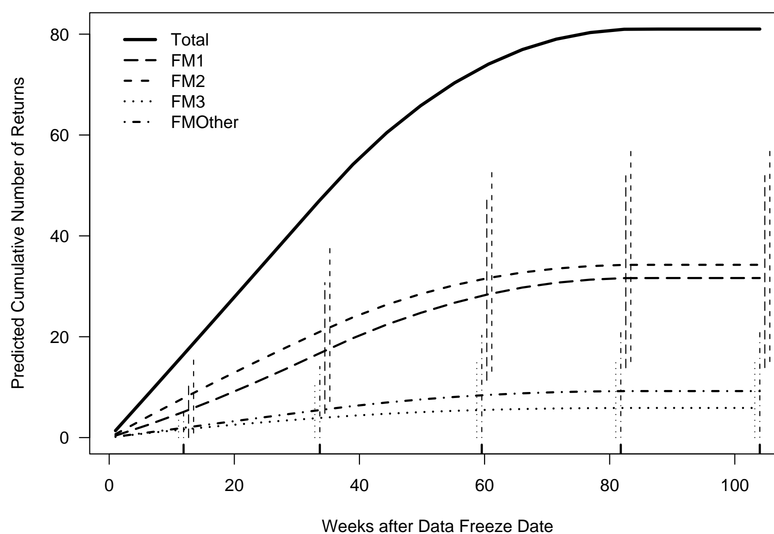

Figure 7: The predicted cumulative number of returns as a function of time for each failure mode for the connected population and the 90% SPIs for the individual failure modes at certain time points. The number of units in the RS at DFD is 912. The vertical segments shows the SPIs for the individual failure modes. There are four segments at each time point. The x-location of these four SPIs are perturbed so that the lines will be visible. The small tick marks inside the plot at the bottom indicate the x-locations of these SPIs.

a single future time are defined as

$$\Pr(\underset{\sim}{N}_k \leq N_k \leq \widetilde{N}_k; k = 1, \cdots, K) = 1 - \alpha.$$

Note that the simultaneousness is over all failure modes not over the time. The naive PIs can be calibrated simultaneously using **Procedure P3** of Appendix A to provide the SPIs. Figure 7 shows the predicted cumulative number of returns as a function of time for each failure mode for the connected population and the 90% SPIs for multiple failure modes at certain time points.

4.1.4 Prediction for the Total Number of Returns

The total number of future returns at s time units after the DFD is $N = \sum_{i \in RS} I_i = \sum_{k=1}^{K} N_k$, where $I_i \sim \text{Bernoulli}(\rho_i)$, $i \in RS$. Here, $\rho_i = \Pr(T_i \leq t_i^w | T_i > t_i, R_i = r_i)$ is the warranty-period-adjusted conditional probability before t_i^w, given use rate r_i. In particular,

$$\rho_i = \frac{F_C(r_i t_i^w; \boldsymbol{\theta}_C) - F_C(r_i t_i; \boldsymbol{\theta}_C)}{1 - F_C(r_i t_i; \boldsymbol{\theta}_C)}. \tag{7}$$

Note also that $\rho_i = \sum_{k=1}^{K} \rho_{ki}$. The ML estimator of ρ_i is $\widehat{\rho}_i$, which can be obtained by substituting the ML estimates $\widehat{\boldsymbol{\theta}}_C$ into (7). We use $\left[\underset{\sim}{N}, \widetilde{N}\right]$ to denote a PI. The naive "plug-in" PI can be obtained by solving $F_N(\underset{\sim}{N}; \widehat{\boldsymbol{\theta}}_C) = \alpha/2$ and $F_N(\widetilde{N}; \widehat{\boldsymbol{\theta}}_C) = 1 - \alpha/2$. Then this PI can be calibrated using **Procedure P1** of Appendix A. Figure 8 shows the point predictions (estimated expected number of returns) and pointwise PIs for the cumulative number of returns as a function of time for the connected units.

4.2 Prediction for the Not-connected Population

For the not-connected population (i.e., that part of the product population without use-rate information), the predictions are also conditional on the observed time in service (t_i) and based on the ML estimators given in Section 3.2.

4.2.1 Prediction for Returns for Individual Failure Modes

To predict the cumulative number of returns for each failure mode, the warranty-period-adjusted conditional failure probability that unit i fails due to failure mode k is

$$\rho_{ki} = \Pr(\Delta_{ki} = 1, T_i \leq t_i^w | T_i > t_i) = \frac{F_T(k, t_i^w; \boldsymbol{\theta}_T) - F_T(k, t_i; \boldsymbol{\theta}_T)}{1 - F_T(t_i; \boldsymbol{\theta}_T)} \quad k = 1, \cdots, K. \tag{8}$$

The ML estimator of ρ_{ki}, denoted by $\widehat{\rho}_{ki}$, can be obtained by evaluating (8) at $\widehat{\boldsymbol{\theta}}_T$. The PI procedure and SPI procedure and their calibrations are similar to that for the connected units

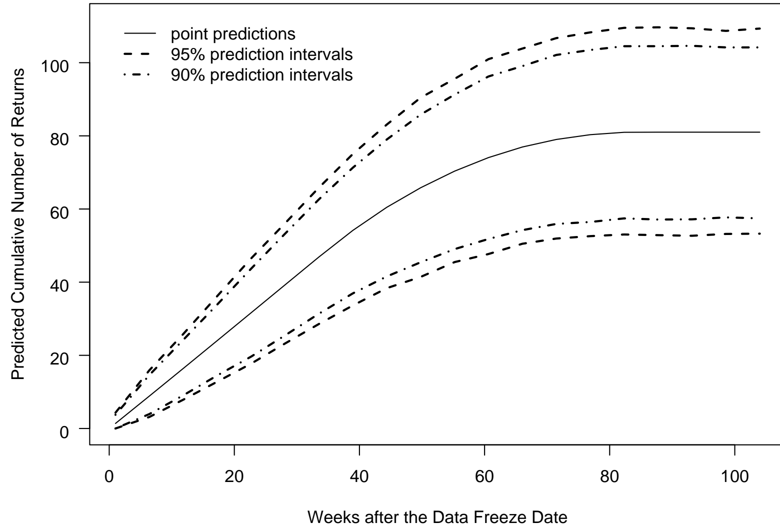

Figure 8: The point predictions and pointwise PIs for the cumulative number of returns as a function of time after the DFD for the connected population.

as described in Sections 4.1.1 and 4.1.3 except that **Procedure P4** of Appendix A should be used to generate the $\widehat{\boldsymbol{\theta}}_T^*$ values. Figure 9 shows the predicted cumulative number of returns as a function of time for each failure mode and 90% SPIs for multiple failure modes at certain time points for the not-connected population.

4.2.2 Prediction for the Total Number of Returns

To predict the total number of returns, the warranty-period-adjusted conditional failure probability is

$$\rho_i = \Pr(T_i \leq t_i^w | T_i > t_i) = \frac{F_T(t_i^w; \boldsymbol{\theta}_T) - F_T(t_i; \boldsymbol{\theta}_T)}{1 - F_T(t_i; \boldsymbol{\theta}_T)}. \tag{9}$$

The ML estimator of ρ_i is $\widehat{\rho}_i$, which can be obtained by evaluating (9) at $\widehat{\boldsymbol{\theta}}_T$. The PI procedure and its calibration are similar to that for the connected units as described in Section 4.1.4 except that **Procedure P4** of Appendix A should be used to generate $\widehat{\boldsymbol{\theta}}_T^*$. Figure 10 shows the point predictions and pointwise PIs for the cumulative number of returns as a function of time for the not-connected population.

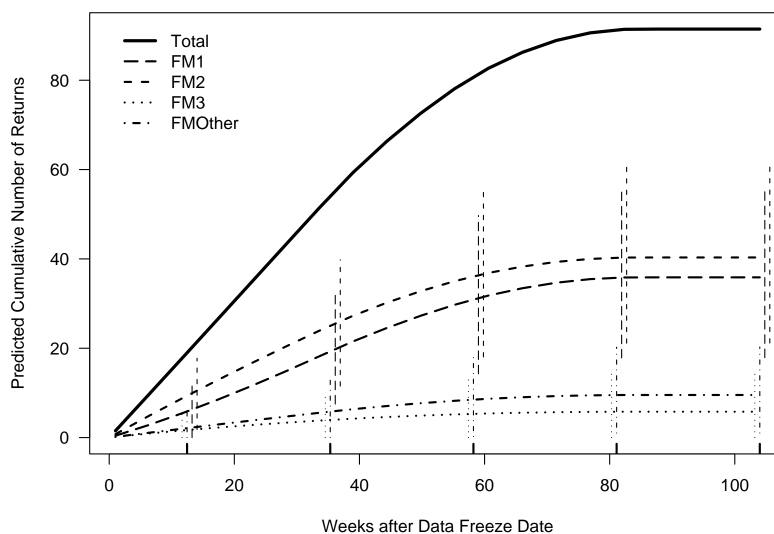

Figure 9: The predicted cumulative number of returns as a function of time for each failure mode for the not-connected population and the 90% SPIs for the individual failure modes at certain time points. The number of units in the RS at DFD is 1038. The vertical segments shows the SPIs for the individual failure modes. There are four segments at each time point. The x-location of these four SPIs are perturbed so that the lines will be visible. The small tick marks inside the plot at the bottom indicate the x-locations of these SPIs.

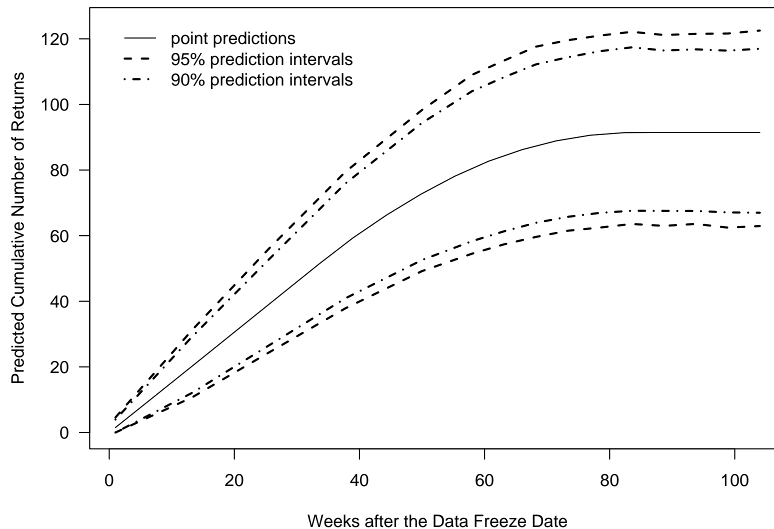

Figure 10: The point predictions and pointwise PIs for the cumulative number of returns as a function of time after the DFD for the not-connected population.

5 Comparison with Traditional Failure-time Data Analysis Approach

In this section, we make comparisons to see some of the advantages of using cycles-to-failure data instead of traditional failure-time data.

5.1 Time-to-Failure Data Prediction Model

For failure-time data with multiple failure modes (t_i, δ_{ki}), the likelihood of the data is

$$L(\boldsymbol{\theta}_T|DATA) = \prod_{k=1}^{K}\prod_{i=1}^{n}\left\{[f_{T_k}(t_i;\boldsymbol{\theta}_{T_k})]^{\delta_{ki}}\,[1 - F_{T_k}(t_i;\boldsymbol{\theta}_{T_k})]^{(1-\delta_{ki})}\right\}.$$

Here $f_{T_k}(\cdot)$ and $F_{T_k}(\cdot)$ are the pdf and cdf of the failure-time distribution. In this analysis, we still use the lognormal distribution for FM1, FM3, and FMOther, and the Weibull distribution for FM2. $\boldsymbol{\theta}_{T_k}$ is the corresponding parameter for failure mode k and $\boldsymbol{\theta}_T = (\boldsymbol{\theta}'_{T_1}, \cdots, \boldsymbol{\theta}'_{T_K})'$. The ML estimator is denoted by $\widehat{\boldsymbol{\theta}}_T$. The predictions and PIs based on the failure-time data can be obtained using procedures similar to those described in Section 4.2.2.

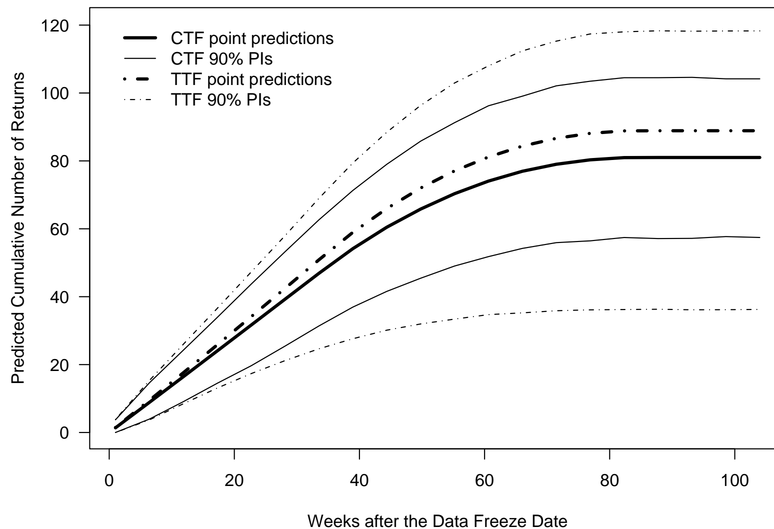

Figure 11: Comparison of prediction result for the failure-time data results and cycles-to-failure data for the connected population.

5.2 Comparisons

Figure 11 shows the point prediction (estimate of the expected number of returns) for the cumulative number of returns and PIs based on the failure-time data and the cycles-to-failure data for the connected population. Figure 12 shows similar results for the not-connected population. The results show that the PIs obtained using the cycles-to-failure information are narrower. For failure-time data, due to censoring, the observed failure times cover a narrow range of the domain of failure-time distribution. The cycles-to-failure data are different. Because some units are heavily used, the observed cycles-to-failure data cover a wider range of the domain of the distribution. Thus, the effective amount of extrapolation needed to make predictions is smaller.

Figures 11 and 12 also show that the point predictions based on failure-time data differ from the point predictions based on cycles-to-failure data but the difference is small relative to the width of the PIs. Also, note that the PIs based on failure-time data are asymmetric which is caused by fact that the bootstrap distribution of $\mu(\widehat{\boldsymbol{\theta}}^{*}_{T})$ is more skewed than that of $\mu(\widehat{\boldsymbol{\theta}}^{*}_{C})$.

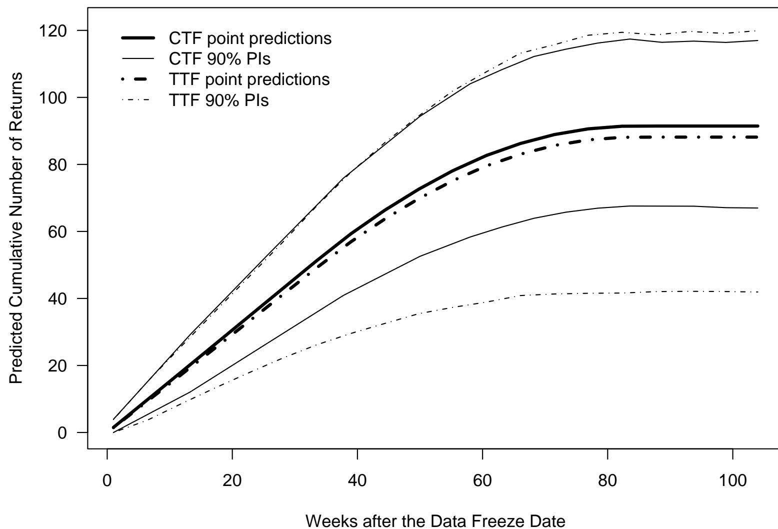

Figure 12: Comparison of prediction result for the failure-time data results and cycles-to-failure data for the not-connected population.

5.3 A Simple Illustrative Example

To obtain broader insights on the advantages of using cycles-to-failure data, we study an example based on a simpler model. Suppose that the distribution of cycles to failure C is lognormal with location parameter μ_C and scale parameter σ_C and that the distribution of use rate R is lognormal with location parameter μ_R and scale parameter σ_R. Because $T = C/R$, the distribution of time to failure is also lognormal with parameters $\mu_T = \mu_C - \mu_R$ and $\sigma_T = \sqrt{\sigma_C^2 + \sigma_R^2}$. Suppose that surviving units are censored at a specified time T_0 (i.e., type I censoring). Thus, the censoring variable for C is $T_0 R$. The variable use-rate results in random censoring for C.

The ML estimator of $\boldsymbol{\theta}_C = (\mu_C, \sigma_C)'$ based on the cycles-to-failure data is denoted by $\widehat{\boldsymbol{\theta}}_C$ and has an asymptotic distribution $N(\boldsymbol{\theta}_C, \Sigma_{\boldsymbol{\theta}_C})$. The ML estimator of $\boldsymbol{\theta}_R = (\mu_R, \sigma_R)'$ based on the use-rate data is denoted by $\widehat{\boldsymbol{\theta}}_R$ and has an asymptotic distribution $N(\boldsymbol{\theta}_R, \Sigma_{\boldsymbol{\theta}_R})$. The ML estimator of $\boldsymbol{\theta}_T = (\mu_T, \sigma_T)'$ based on the time-to-failure data is denoted by $\boldsymbol{\theta}_T = (\widehat{\mu}_T, \widehat{\sigma}_T)$ and has an asymptotic distribution $N(\boldsymbol{\theta}_T, \Sigma_{\boldsymbol{\theta}_T})$.

To see the advantages of using the use-rate model, we will compare the approximate large-sample variance of the two different ML estimators of t_p, the p quantile of the failure-time distribution. The ML estimator based on the traditional failure-time data is $\widehat{t}_p = \widehat{\mu}_T + z_p\widehat{\sigma}_T$. The ML estimator based on combination of the cycles-to-failure data and the use-rate data is

$\widehat{t}_p = \widehat{\mu}_C - \widehat{\mu}_R + z_p\sqrt{\widehat{\sigma}_C^2 + \widehat{\sigma}_R^2}$. Here z_p is the p quantile of the standard normal distribution. We evaluate in the ratio of the approximate large-sample variances of these two estimators,

$$VR = \frac{(1, z_p)\Sigma_T(1, z_p)'}{(1, \rho_C z_p)\Sigma_C(1, \rho_C z_p)' + (-1, \rho_R z_p)\Sigma_R(-1, \rho_R z_p)'},$$

where $\rho_C = \sigma_C/\sqrt{\sigma_C^2 + \sigma_R^2}$ and $\rho_R = \sigma_R/\sqrt{\sigma_C^2 + \sigma_R^2}$. The details of how we compute the approximate large-sample variance matrices $\Sigma_{\boldsymbol{\theta}_C}, \Sigma_{\boldsymbol{\theta}_R}$, and $\Sigma_{\boldsymbol{\theta}_T}$ are given in Appendix B.

Figure 13 shows VR versus p for different percentages failing. We chose $\boldsymbol{\theta}_C = (8.22, 0.74)'$ and $\boldsymbol{\theta}_R = (1.61, 0.99)'$, which are based on estimates from Product D in this paper. Figure 13 shows that except for one case, $VR > 1$. This implies that the estimator based on the cycles-to-failure data outperforms the estimator based on the traditional failure-time data. We also observe that VR tends to be larger when the percentage failing is small and VR is decreasing when the percentage failing is increasing. For a given failing percentage, the VR is larger on the right side than that on the left side. This is because there is more extrapolation on the right side. The minimum of each VR curve is also decreasing as the percentage failing increases. Interestingly, the minimum of VR when the percentage failing is 1% occurs approximately where $p = 0.01$. This is because, for failure-time data, the amount of extrapolation needed to estimate the 0.01 quantile is approximately minimum when the percentage failing is 1%. It can also be shown that the minimum of VR is 1 when the data are complete (no censoring) and that this minimum is reached when $p = 0.5$. This is because when the data are complete, there is no extrapolation and the approximate large-sample variance of $\widehat{t}_p$ is minimized for the lognormal distribution when $p = 0.5$.

6 Conclusions and Areas for Future Research

In this paper, we have developed models and methods to incorporate auxiliary use-rate information that arises in field reliability data for some products. Our application focuses on returns predictions of a particular product, Product D. We also show that there are important advantages to using a model based on cycles to failure. That is, the prediction based on the cycles-to-failure data is more accurate in terms of the width of the PIs and, generally requires less extrapolation. We expect data of this kind will be more widely available in the future due to the changes in technology.

The following are areas for related future research.

- In some applications, it is possible to download the use rate as a time series for each unit. A different model will be needed to analyze failure-time data with use-rate time series. The cumulative exposure model in Nelson (2001) could be useful for this type of

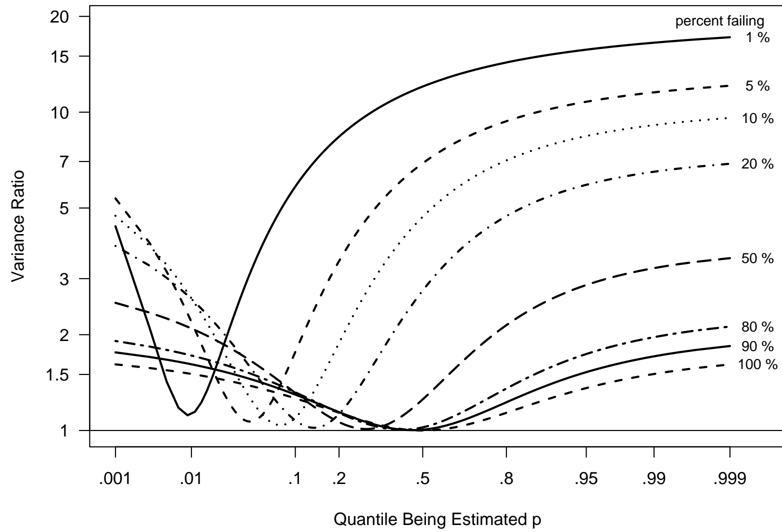

Figure 13: Comparisons of the asymptotic variance ratio for estimating lognormal t_p for different percentage failing.

data. Extensions of the cumulative exposure model, however, are needed to handle the multiple failure modes and PI calibration.

- It is also possible, in some applications, to obtain dynamic information on more variables, such as the environmental temperature, humidity, and load. Other products, for example, high-voltage power transformers can have tremendous amounts of variation in ambient temperature/environment and load at different locations and in different seasons. Appropriate regression models could be used for such explanatory seasonal variables.

- Degradation data are another type of data that are used to make predictions for field reliability of products. Modern sensor technology can provide degradation measurements (or indirect measurements) for products or components of products and this data will often be available dynamically. For example, sensors installed on the airplane wings can monitor such variables as air pressure and stress. Such information could be used to develop models for the health status of the airplane wings.

- Bayesian methods have been used in warranty predictions (e.g., Stephens and Crowder 2004). In some applications, there may be important prior information on some model parameters. Then combining the prior information and the dynamic information about the product has the potential to provide more accurate prediction results.

Acknowledgments

The work in this paper was partially supported by funds from NSF Award CNS0540293 to Iowa State University. We would also like to thank Katherine Meeker and Ye Tian for helpful comments on an earlier version of this paper.

A Prediction Interval Calibration

Here we describe procedures for the calibration of the PIs. These procedures are similar to those used in Hong, Meeker, and McCalley (2009), but were customized for this application.

A.1 Procedure P1 for Calibrating PIs for the Cumulative Number of Returns

The calibrated PI, $\left[\underset{\sim}{N}_k, \widetilde{N}_k\right]$ for the cumulative number of returns for failure mode k at a specified date in the future can be obtained by using the following procedure.

Procedure P1:

1. Simulate I^*_{ki} from Bernoulli$(\widehat{\rho}_{ki})$, $i \in RS$ and compute $N^*_k = \sum_{i \in RS} I^*_{ki}$.
2. Repeat step 1 B times to get $N^*_{kb}, b = 1, 2, \cdots, B$.
3. Obtain $\widehat{\boldsymbol{\theta}}^*_{Cb}, b = 1, 2, \cdots, B$ using **Procedure P2**.
4. Compute $U^*_{kb} = F_{N_k}(N^*_{kb}; \widehat{\boldsymbol{\theta}}^*_{Cb}), b = 1, 2, \cdots, B$.
5. Let $u^l_{N_k}, u^u_{N_k}$ be, respectively, the lower and upper $\alpha/2$ sample quantiles of $U^*_{kb}, b = 1, \cdots, B$. The $100(1-\alpha)\%$ calibrated prediction interval can obtained by solving for $\underset{\sim}{N}_k$ and $\widetilde{N}_k$ in $F_{N_k}(\underset{\sim}{N}_k; \widehat{\boldsymbol{\theta}}_C) = u^l_{N_k}$ and $F_{N_k}(\widetilde{N}_k; \widehat{\boldsymbol{\theta}}_C) = u^u_{N_k}$, respectively.

The uncertainty in $\widehat{\boldsymbol{\theta}}_C$ is accounted for by the bootstrap obtained by using **Procedure P2**.

A.2 Procedure P2 for Computing Bootstrap Estimates for the Connected Population

Bootstrap parameter estimates $\widehat{\boldsymbol{\theta}}^*_{Cb}, b = 1, 2, \cdots, B$ are needed in Sections 4.1.2 through 4.1.4 for use in **Procedures P1** and **P3**. **Procedure P2** is similar to that used in Hong, Meeker, and McCalley (2009), and is used to obtain the $\widehat{\boldsymbol{\theta}}^*_{Cb}$ values using the random weighted likelihood bootstrap which was introduced by Newton and Raftery (1994).

Procedure P2:

1. Simulate random values $Z_i, i = 1, 2, \cdots, n$ that are *i.i.d.* from a distribution having the property $\mathrm{E}(Z_i) = [\mathrm{Var}(Z_i)]^{1/2}$.

2. The random weighted likelihood is $L^*_{CTF}(\boldsymbol{\theta}_C|DATA) = \prod_{i=1}^{n} [L_i(\boldsymbol{\theta}_C|DATA)]^{Z_i}$ where $L_i = \prod_{k=1}^{K} \left\{ [f_{C_k}(c_i; \boldsymbol{\theta}_{C_k})]^{\delta_{ki}} [1 - F_{C_k}(c_i; \boldsymbol{\theta}_{C_k})]^{(1-\delta_{ki})} \right\}$ is the likelihood contribution from an individual observation.

3. Obtain the ML estimate $\widehat{\boldsymbol{\theta}}^*_C$ by maximizing $L^*_{CTF}(\boldsymbol{\theta}_C|DATA)$.

4. Repeat step 1-3 B times, to get B bootstrap samples $\widehat{\boldsymbol{\theta}}^*_{Cb}, b = 1, 2, \cdots, B$.

The distribution of Z_i is chosen as exponential(1) for this application. See, Hong, Meeker, and McCalley (2009) for a discussion of the effect of the distribution of Z_i.

A.3 Procedure P3 for Calibrating Simultaneous PIs for the Cumulative Number of Returns

The following procedure is used for the calibration of SPI in Section 4.1.3.

Procedure P3:

1. Simulate $(I^*_{1i}, I^*_{2i}, \cdots, I^*_{Ki})'$ from a Multinominal$(1; \widehat{\rho}_{1i}, \widehat{\rho}_{2i}, \cdots, \widehat{\rho}_{Ki})$ distribution for each i in the RS.

2. Obtain $(N^*_1, N^*_2, \cdots, N^*_K)'$ by $N^*_k = \sum_{i \in RS} I^*_{ki}, k = 1, 2, \cdots, K$.

3. Repeat 1-2 B times to get $(N^*_{1b}, N^*_{2b}, \cdots, N^*_{Kb})', b = 1, 2, \cdots, B$.

4. Obtain $\widehat{\boldsymbol{\theta}}^*_{Cb}, b = 1, 2, \cdots, B$ using **Procedure P2**.

5. For a certain α and $b = 1, 2, \cdots, B$, solve $\underset{\sim}{N}^*_{kb}$ and $\widetilde{N}^*_{kb}$, $k = 1, \cdots, K$ from (6) after replacing $\widehat{\boldsymbol{\theta}}_C$ with $\widehat{\boldsymbol{\theta}}^*_{Cb}$. If $\underset{\sim}{N}^*_{kb} \leq N^*_{kb} \leq \widetilde{N}^*_{kb}$ holds for all k, we call a success. Denote the fraction of successes by $cp(\alpha)$.

6. Repeat 5 for α over a certain range and solve $cp(\alpha) = \alpha_0$ for the nominal α where α_0 is the desired CP.

A.4 Procedure P4 for Computing Bootstrap Estimates for the Not-connected Population

In Sections 4.2.1 and 4.2.2, $\widehat{\boldsymbol{\theta}}^*_{Tb}, b = 1, 2, \cdots, B$ are needed. To get $\widehat{\boldsymbol{\theta}}^*_{Tb}$ using the random weighted likelihood bootstrap, we use the following procedure.

Procedure P4:

1. Simulate random values $Z_i, i = 1, 2, \cdots, n$ and $Z_j, j = 1, 2, \cdots, m$ that are *i.i.d.*
2. Obtain the random weighted estimator of $F_{\tau R}$,
$$\widehat{F}^*_{\tau R}(r) = (\sum_{i=1}^{n} Z_i)^{-1} \sum_{i=1}^{n} Z_i \mathbf{1}_{(r_i \le r/\tau)}.$$
3. The random weighted likelihood is
$$L^*(\boldsymbol{\theta}_C, \widehat{F}^*_{\tau R}|DATA) = L^*_{CTF}(\boldsymbol{\theta}_C|DATA) \times L^*_{TIS}(\boldsymbol{\theta}_C, \widehat{F}^*_{\tau R}|DATA).$$
Here, $L^*_{CTF}(\boldsymbol{\theta}_C|DATA)$ is the same as in Step 2 of **Procedure P2** and
$$L^*_{TIS}(\boldsymbol{\theta}_C, \widehat{F}^*_{\tau R}|DATA) = \prod_{j=1}^{m} \left[L_j(\boldsymbol{\theta}_C, \widehat{F}^*_{\tau R}|DATA)\right]^{Z_j}$$
where $L_j = \left(\prod_{k=1}^{K} \left[A_{kj}(t_j; \boldsymbol{\theta}_C, \widehat{F}^*_{\tau R})\right]^{\delta_{kj}}\right) \times \left[1 - F_T(t_j; \boldsymbol{\theta}_C, \widehat{F}^*_{\tau R})\right]^{\prod_{k=1}^{K}(1-\delta_{kj})}.$
4. Obtain the ML estimate $\widehat{\boldsymbol{\theta}}^*_T$ by maximizing $L^*(\boldsymbol{\theta}_C, \widehat{F}^*_{\tau R}|DATA)$.
5. Repeat step 1-4 B times, to get B bootstrap samples $\widehat{\boldsymbol{\theta}}^*_{Tb}, b = 1, 2, \cdots, B$.

B Approximate Large-sample Variance Matrices for the Illustrative Example

This appendix shows the computation of the asymptotic variance matrices that are used in Section 5.3. The asymptotic variance matrices can be obtained as the inverse of the corresponding Fisher information matrices. That is $\Sigma_{\boldsymbol{\theta}_C} = I^{-1}_{\boldsymbol{\theta}_C}$, $\Sigma_{\boldsymbol{\theta}_R} = I^{-1}_{\boldsymbol{\theta}_R}$ and $\Sigma_{\boldsymbol{\theta}_T} = I^{-1}_{\boldsymbol{\theta}_T}$, where $I_{\boldsymbol{\theta}_C}$, $I_{\boldsymbol{\theta}_R}$ and $I_{\boldsymbol{\theta}_T}$ are the corresponding Fisher information matrices. In particular, $I_{\boldsymbol{\theta}_R} = (n/\sigma^2_R)\,\mathrm{diag}(1, 2)$. Here n is the number of observations. Let $y_0 = \log(T_0)$ be the logarithm of the censoring time for Type I censoring. Then,
$$I_{\boldsymbol{\theta}_T} = \frac{n}{\sigma^2_T} \begin{pmatrix} f_{11}\left[\frac{y_0-\mu_T}{\sigma_T}\right] & f_{12}\left[\frac{y_0-\mu_T}{\sigma_T}\right] \\ f_{12}\left[\frac{y_0-\mu_T}{\sigma_T}\right] & f_{22}\left[\frac{y_0-\mu_T}{\sigma_T}\right] \end{pmatrix}.$$
Here f_{11}, f_{12} and f_{22} are elements that can be computed by the algorithm in Escobar and Meeker (1994). Because C is randomly censored by T_0R, the Fisher information is
$$I_{\boldsymbol{\theta}_C} = \frac{n}{\sigma^2_C} \begin{pmatrix} \int_{-\infty}^{\infty} f_{11}\left[\frac{x-\mu_T}{\sigma_T}\right] h(x)dx & \int_{-\infty}^{\infty} f_{12}\left[\frac{x-\mu_T}{\sigma_T}\right] h(x)dx \\ \int_{-\infty}^{\infty} f_{12}\left[\frac{x-\mu_T}{\sigma_T}\right] h(x)dx & \int_{-\infty}^{\infty} f_{22}\left[\frac{x-\mu_T}{\sigma_T}\right] h(x)dx \end{pmatrix}.$$
Here $h(x)$ is the density of a normal distribution with location $\log(T_0)+\mu_R$ and scale σ_R. More details of computing the Fisher information matrix under random censoring can be found at Escobar and Meeker (1998).

References

Barndorff-Nielsen, O. and D. Cox (1996). Prediction and asymptotics. *Bernoulli,* 2, 319–340.

Beran, R. (1990). Calibrating prediction regions. *Journal of the American Statistical Association,* 85, 715–723.

Crowder, M. J. (2001). *Classical Competing Risks.* Boca Raton, FL: Chapman & Hall/CRC.

David, H. A. and M. L. Moeschberger (1978). *The Theory of Competing Risks.* London: Griffin.

Escobar, L. A. and W. Q. Meeker (1994). Fisher information matrix for the extreme value, normal and logistic distribtions and censored data. *Applied Statistics,* 43, 533–540.

Escobar, L. A. and W. Q. Meeker (1998). Fisher information matrices with censoring, truncation, and explanatory variables. *Statistica Sinica,* 8, 221–237.

Escobar, L. A. and W. Q. Meeker (1999). Statistical prediction based on censored life data. *Technometrics,* 41, 113–124.

Escobar, L. A. and W. Q. Meeker (2006). A review of accelerated test models. *Statistical Science,* 21, 552–577.

Hong, Y., W. Q. Meeker, and J. D. McCalley (2009). Prediction of remaining life of power transformers based on left truncated and right censored lifetime data. *The Annals of Applied Statistics,* 3, in press.

Kalbfleisch, J. D., J. F. Lawless, and J. A. Robinson (1991). Methods for the analysis and prediction of warranty claims. *Technometrics,* 33, 273–285.

Komaki, F. (1996). On asymptotic properties of predictive distributions. *Biometrika,* 83, 299–313.

Lawless, J. F. (1998). Statistical analysis of product warranty data. *International Statistical Review,* 66, 41–60.

Lawless, J. F. (2003). *Statistical Models and Methods for Lifetime Data* (2nd edition). Hoboken, NJ: John Wiley & Sons, Inc.

Lawless, J. F., M. J. Crowder, and K. A. Lee (2009). Analysis of reliability and warranty claims in products with age and usage scales. *Technometrics,* 51, 14–24.

Lawless, J. F. and M. Fredette (2005). Frequentist prediction intervals and predictive distributions. *Biometrika,* 92, 529–542.

Meeker, W. Q. and L. A. Escobar (1998). *Statistical Methods for Reliability Data.* New York: John Wiley & Sons, Inc.

Meeker, W. Q., L. A. Escobar, and Y. Hong (2009). Using accelerated life tests results to predict product field reliability. *Technometrics,* 51, 146–161.

Nelson, W. (2001). Prediction of field reliability of units, each under differing dynamic stresses, from accelerated test data. *Handbook of Statistics 20: Advances in Reliability, Chapter IX*. Amsterdam: North-Holland.

Newton, M. A. and A. E. Raftery (1994). Approximate Bayesian inference with the weighted likelihood bootstrap. *Journal of the Royal Statistical Society: Series B,* 56, 3–48.

Stephens, D. and M. Crowder (2004). Bayesian analysis of discrete time warranty data. *Applied Statistics,* 53, 195–217.

Volkova, A. Y. (1996). A refinement of the central limit theorem for sums of independent random indicators. *Theory of Probability and its Applications,* 40, 791–794.

Yang, G. (2007). *Life Cycle Reliability Engineering.* Hoboken, NJ: John Wiley & Sons, Inc.